Available online at www.sciencedirect.com
ScienceDirect
Analytica Chimica Acta 581 (2007) 193–201
ANALYTICA CHIMICA ACTA
www.elsevier.com/locate/aca

Towards multi-colour strategies for the detection of oligonucleotide hybridization using quantum dots as energy donors in fluorescence resonance energy transfer (FRET)

W. Russ Algar, Ulrich J. Krull *

Chemical Sensors Group, Department of Chemical and Physical Sciences, University of Toronto at Mississauga, 3359 Mississauga Road North, Mississauga, Ontario L5L 1C6, Canada

Received 26 June 2006; received in revised form 14 August 2006; accepted 14 August 2006
Available online 22 August 2006

Abstract

The potential for a simultaneous two-colour diagnostic scheme for nucleic acids operating on the basis of fluorescence resonance energy transfer (FRET) has been demonstrated. Upon ultraviolet excitation, two-colours of CdSe/ZnS quantum dots with conjugated oligonucleotide probes act as energy donors yielding FRET-sensitized acceptor emission upon hybridization with fluorophore (Cy3 and Alexa647) labeled target oligonucleotides. Energy transfer efficiencies, Förster distances, changes in quantum yield and lifetime, and signal-to-noise with respect to non-specific adsorption have been investigated. The dynamic range and limit-of-detection are tunable with the concentration of QD–DNA conjugate. The Cy3 and Alexa647 acceptor schemes can detect target from 4 to 100% or 10 to 100% of the QD–DNA conjugate concentration, respectively. Nanomolar limits of detection have been demonstrated in this paper, however, results indicate that picomolar detection limits can be achieved with standard instrumentation. The use of an intercalating dye (ethidium bromide) as an acceptor to alleviate non-specific adsorption is also described and increases signal-to-noise from S/N < 2 to S/N = 9–10. The ethidium bromide system had a dynamic range from 8 to 100% of the QD–DNA conjugate concentration and could detect target in a matrix containing an excess of non-complementary nucleic acid.

Keywords: Quantum dots; Energy transfer; Deoxyribonucleic acid; Ethidium bromide; Biosensor

1. Introduction

Quantum dots (QDs), or colloidal semiconductor nanocrystals, have been the center of much attention in the past few years. The unique photophysical properties of these particles, particularly in terms of brightness, photostability, narrow tunable emission, and broad absorption, are attractive in many applications. One area of application has been imaging with quantum dots [1–6], where the optical properties are advantageous in comparison to most organic fluorophores. Another growing area of application has been diagnostics. For example, antibodies have been conjugated to quantum dots for use in sandwich immunoassays [7], and in fluorescence resonance energy transfer (FRET) based sensors for 2,4,6-trinitrotoluene (TNT) [8]. In other FRET motifs, quantum dots have been conjugated to DNA hairpins for use in molecular beacons [9], have been used to detect hybridization events [10–12], and have also been conjugated to peptides and proteins for detection of enzymes [13] and small molecules [14]. We report an initial investigation of the development of a FRET and QD-based strategy for the detection of nucleic acids, with the long term goal of achieving a multi-colour diagnostic technology suitable for the simultaneous detection of multiple sequences.

In general, most multi-colour optical diagnostic or imaging schemes require multiple excitation sources. One of the more popular optical diagnostic schemes for nucleic acid detection is fiber-optic biosensors, which have been developed for the detection of pathogens [15,16] and genetic analyses [17,18]. However, the simultaneous detection of multiple sequences requires either two-colour excitation or discrete sensor elements exposed to a common analyte solution. Other conventional optical technologies for multiplexed analysis, including both fluorescence and surface plasmon resonance (SPR) imaging of nucleic acid microarrays, require fabrication of discrete sensing elements

* Corresponding author. Tel.: +1 905 828 5437; fax: +1 905 828 5425.
E-mail address: ukrull@utm.utoronto.ca (U.J. Krull).

0003-2670/$ – see front matter © 2006 Elsevier B.V. All rights reserved.
doi:10.1016/j.aca.2006.08.026

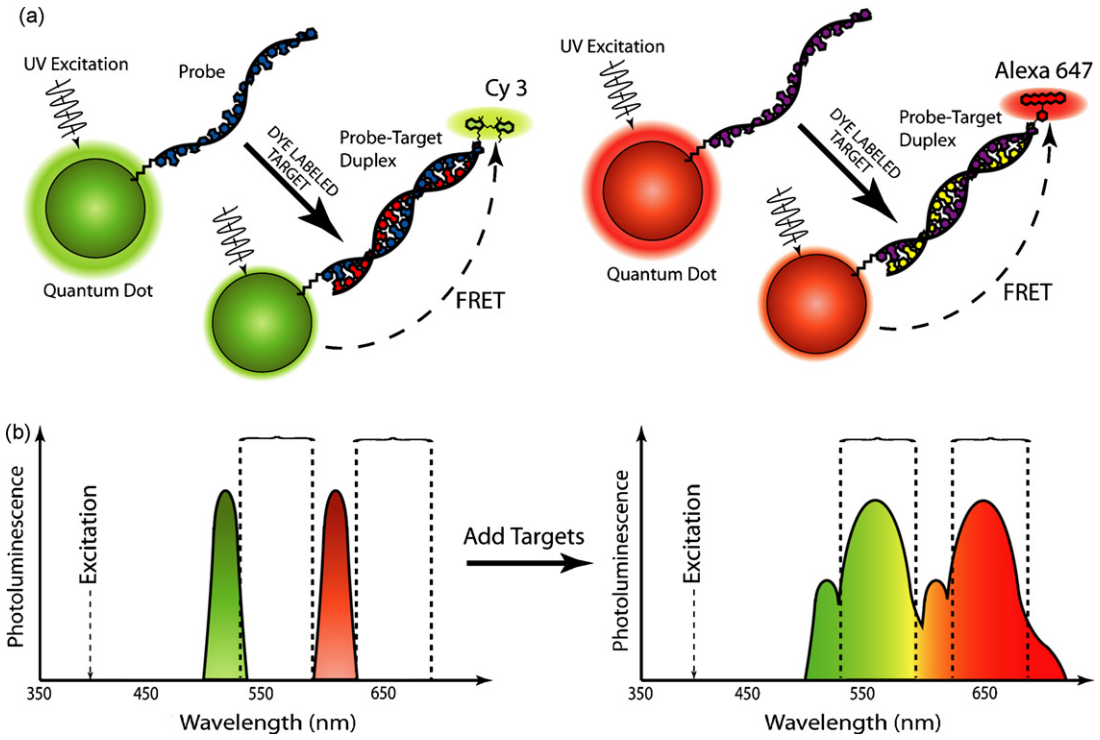

Fig. 1. Proposed QD–FRET-based strategy for two-colour nucleic acid detection. (a) Simultaneous and efficient excitation of green and red quantum dots was possible in the ultraviolet-region without significant excitation of Cy3 or Alexa647 in solution. When probe oligonucleotides were conjugated to QDs, hybridization with a Cy3 or Alexa647 labeled target oligonucleotide yielded FRET-sensitized emission from the dyes, which was used as the analytical signal. The green QD–Cy3 FRET pair utilized the SMN1 sequence and the red QD–Alexa647 pair utilized the LacZ sequence. (b) A cartoon of the expected emission profiles, where the bracketed regions are of particular analytical interest. (For interpretation of the references to colour in this figure legend, the reader is referred to the web version of the article.)

(spots) [19–25]. Techniques based on encoded microspheres, including those encoded with QDs, have recently allowed multiplexed analyses of nucleic acids using a single excitation source, but require observation of individual microspheres, typically by flow cytometry [26–30]. By combining the broad absorption spectra of quantum dots with stimulated emission via FRET, the new work reported herein has developed an approach to multi-colour nucleic acid diagnostics which uses only a single excitation source, permits bulk measurements, and does not require discrete sensing elements for each target. Multiplexed schemes combining FRET with quantum dots have been characterized [31] and applied [7] to non-nucleic acid targets previously. However, in these cases the acceptor species was a dark quencher rather than a fluorophore. Although effective, the approach using a quencher may be susceptible to non-FRET mechanisms of luminescence quenching, potentially resulting in spurious signals. The proposed emission scheme is advantageous in that only close proximity between the acceptor and the donor QD can result in emission via FRET.

Using a single excitation wavelength near the ultraviolet region of the spectrum, different sizes of QDs can be simultaneously excited due to their broad absorption spectra. In this work, smaller green emitting QDs are conjugated to probe oligonucleotides that are complementary to target sequences diagnostic of a genetic disorder (spinal muscular atrophy). Similarly, larger red emitting QDs are conjugated to probes diagnostic of a pathogen (*E. coli*). Upon hybridization of the green and red QD–DNA conjugates with target sequences labeled with Cyanine 3 (Cy3) and Alexa Fluor 647 (Alexa647), respectively, the QDs act as energy donors. As shown in Fig. 1, the result is simultaneous FRET-sensitized emission from the Cy3 and Alexa647 acceptor dyes. Aside from the ability to perform multi-colour analyses on a single sensor element with a single excitation source, the resistance of this scheme to photobleaching is similar to that of QDs since the organic fluorophores are excited indirectly via FRET. This work provides demonstration of proof-of-principle for both single-colour and two-colour analyses in solution phase experiments using a sensitized emission scheme. The quantum yields and photoluminescence lifetimes of QD–DNA conjugates in this system are characterized. Non-specific adsorption of oligonucleotides on the QD surface leading to FRET is encountered, however, the use of an intercalating dye such as ethidium bromide is shown to alleviate this issue. Aside from their inherent selectivity for double-stranded DNA, intercalating dyes may also be a better pragmatic approach since they avoid labeling of target material.

2. Experimental

2.1. Reagents and oligonucleotides

Adirondrack Green and Maple Red CdSe/ZnS core/shell semiconductor nanocrystals (QDs) in toluene were from Evident Technologies (Troy, NY, USA). Ninety-eight percent mercaptoacetic acid, 99.5% *N*,*N*-diisopropylethylamine, and *N*-(3-dimethylaminopropyl)-*N*′-ethylcarbodiimide hydrochloride

Table 1
Oligonucleotide sequences used in hybridization assays

Oligonucleotide	Sequence
Green QD-SMN1	
Probe	$NH_2C_6H_{12}$-5′-ATT TTG TCT GAA ACC CTG T-3′
Target-Cy3	Cy3-5′-ACA GGG TTT CAG ACA AAA T-3′
Target	5′-ACA GGG TTT CAG ACA AAA T-3′
Red QD-LacZ	
Probe	$NH_2C_6H_{12}$-5′-CTT ACT TCC ATG ATT TCT TTA ACT-3′
Target-Alexa647	Alexa647-5′-AGT TAA AGA AAT CAT GGA AGT AAG-3′

(EDC) were from Sigma–Aldrich (Oakville, Ont., Canada) and used without further purification. Chloroform was from EM Science (Toronto, Ont., Canada) and used as received.

Modified and unmodified oligonucleotides were from Integrated DNA Technologies (Coralville, IA, USA) and were HPLC purified by the manufacturer. The oligonucleotides were dissolved in deionized water with a specific resistance of 18 MΩ cm^{-1}. Nucleotide sequences are listed in Table 1. Ethidium bromide homodimer was obtained from Sigma–Aldrich. Water was deionized and purified by the Milli-Q cartridge purification system (Millipore Corp., Mississauga, Ont., Canada). Tris–borate (TB, 90 mM, pH 7.4) buffer solutions were prepared with autoclaved double-distilled water and filtered through a 0.2 μm syringe filter for the preparation of QD solutions.

2.2. Instruments

Ultraviolet–visible absorption spectra were measured using a Libra S22 spectrometer (Bichrom Ltd., Cambridge, UK) and a HP 8452A Diode-Array Spectrometer (Hewlett Packard Corporation, Palo Alto, CA, USA). Solution phase fluorescence spectra were measured using a QuantaMaster PTI Spectrofluorimeter and Felix Software (Photon Technology International, Lawrenceville, NJ, USA). Photoluminescence lifetime measurements were made using a time correlated single photon counter (constructed in-house), driven by a 520 nm femtosecond laser (pulse duration: 200 fs, repetition rate: 15 MHz, bandwidth: 3 nm, mean power: 1 mW at 520 nm).

2.3. Quantum dot surface modification and preparation of DNA conjugates

QDs in toluene were made water soluble by ligand exchange with mercaptoacetic acid (MAA). In a typical procedure, QDs in toluene were diluted in chloroform with >5 × 10^4-fold excess of MAA and sufficient *N*,*N*-diisopropylethylamine to render the solution basic. The mixture was sonicated for 2–3 min and refluxed under argon for 8–12 h. During this period the quantum dots precipitated. As has been reported elsewhere [32], the heating was found to be essential for producing dots that could withstand purification. The precipitate and supernatant were centrifuged to produce a compact pellet, the supernatant discarded, and the precipitate was washed three times with chloroform. Each wash consisted of mixing, centrifuging, and discarding the supernatant. After drying in air to remove residual chloroform, the precipitate was dissolved in TB buffer. This was followed by re-precipitation via the addition of 95% ethanol (*ca*. 3:1 EtOH:TB) and centrifugation. This step was repeated once more prior to dissolving the water soluble quantum dots (MAA–QDs) in the desired amount of TB buffer. The concentration of MAA–QDs was determined by absorption spectroscopy using the first absorption peak (green = 515 nm; red = 600 nm). Typical recoveries from ligand exchange were 80–90%, with the larger red QDs having higher recoveries.

DNA conjugates were prepared by mixing MAA–QDs with n = 1 or 2 equiv. of amine modified oligonucleotides in TB buffer containing EDC. Reaction mixtures were generally 5–20 μM in QDs and allowed to stand 6–8 h at room temperature. It should be noted that phosphate buffers commonly used with oligonucleotides interfered with the coupling reaction. Following the reaction, excess EDC was removed by precipitation of the QD–DNA conjugate with ethanol, centrifugation, and discarding the supernatant. The conjugates were then redissolved in TB buffer and precipitated with ethanol twice more before finally dissolving in the desired amount of buffer. The probe-to-QD ratio was controlled by the stoichiometry of the EDC coupling reaction. The properties of the resulting conjugates were assumed to be dominated by a large population of QD–n × DNA conjugates with minimal influence from the potential existence of small QD–($n \pm 1$) × DNA conjugate populations. Typical conjugate recoveries were 70–80% and final concentrations were determined by UV–visible absorption spectroscopy. As reported elsewhere [33], we found that the QDs were susceptible to aggregation during the EDC coupling reaction. This appeared to be a function of the amount of EDC, and was ameliorated by reducing the quantity of EDC in solution, albeit still working with a 10^4 to 10^5-fold excess. Green QD–DNA conjugates were centrifuged for 15 min at 10 000 rpm; red QD–DNA conjugates were centrifuged for 6–8 min at 6000 rpm. The latter was required due to the greater instability of the red QDs, which would not consistently re-disperse if centrifuged too vigorously.

2.4. Determining quantum yields, lifetimes, and Förster distances

The Förster distance, Eq. (1), is a characteristic of a donor–acceptor pair, and depends on factors including the refractive index of the surrounding medium, n, the donor quantum yield, Φ_D, the relative orientation between donor emission and acceptor absorption dipoles, and the degree of spectral resonance between the two species [34]. These latter two parameters are described by the orientation factor, κ^2, and spectral overlap integral, J, respectively. The spectral overlap integral, Eq. (2), is a function of the fluorescence intensity of the donor, F_D, and molar absorptivity of acceptor, ε_A, as a function of wavelength, λ, normalized against the total donor emission [34]. Acceptor ultraviolet–visible absorption and donor fluorescence emission spectra were obtained with 3 μM solutions of oligonucleotide, and 10 μM (green) and 1.0 μM (red) solutions of QD, respectively. From the spectra obtained, the integrands in Eq. (2) were

calculated at 0.5 nm increments and integrated numerically to determine the spectral overlap.

$$R_o^6 = 8.79 \times 10^{-28}\,\text{mol} \times (n^{-4}\kappa^2\Phi_D J) \quad (1)$$

$$J = \frac{\int F_D(\lambda)\varepsilon_A(\lambda)\lambda^4\,d\lambda}{\int F_D(\lambda)\,d\lambda} \quad (2)$$

Quantum yield values for QDs were determined relative to fluorescein dye in sodium borate buffer fixed at pH 9.5. The quantum yield of fluorescein under these conditions is known to be 0.93 [35] and the quantum yield, Φ, of QDs were determined as a ratio, Eq. (3a), of their integrated emission, $F\,d\lambda$, corrected for different molar absorptivities at the wavelength of excitation, ε, and for concentration, c. Fluorescein was excited at 490 nm. To minimize error, fluorescence and absorbance, A, were measured from the same aliquot of solution, in which case Eq. (3a) reduces to Eq. (3b) via Beer's law. A consistent path length is assumed in both equations.

$$\frac{\int F\,d\lambda}{\int F_{ref}\,d\lambda} = \frac{\varepsilon}{\varepsilon_{ref}}\frac{\Phi}{\Phi_{ref}}\frac{c}{c_{ref}} \quad (3a)$$

$$\Phi = \Phi_{ref}\frac{\int F\,d\lambda}{A}\frac{A_{ref}}{\int F_{ref}\,d\lambda} \quad (3b)$$

Photoluminescence lifetimes were measured using 1.0 or 0.06 μM solutions of the desired green or red QD/QD–DNA conjugate, respectively. Decay curves were obtained using SPCM software (Version 8.50) and SPC-630 hardware (Becker & Hickl GmbH, Berlin, Germany), and analyzed using SPCImage (Version 2.8.3.2921, Becker & Hickl GmbH). Decay curves were fit with a monoexponential lifetime by minimizing the χ^2 value. The system response used in the fitting routine was measured experimentally. A monoexponential decay fit the data well and simplified analysis of the FRET efficiency. The emission of the green QD was isolated by using a combination of a 530 nm long-pass coloured glass filter (Melles Griot, Rochester, NY, USA) and 550 nm short-pass interference filter (ThorLabs, Newton, NJ, USA). Using a spectrofluorimeter, this was confirmed to block the majority of the Cy3 or ethidium bromide emission excited directly at 520 nm. The red QD emission was isolated using a combination of a 590 nm long-pass filter (Nikon, Kawaski, Japan) and a 650 nm short-pass interference filter (ThorLabs).

2.5. Hybridization assays

For single-colour experiments, green QD–1 × DNA and red QD–2 × DNA conjugates were prepared using the probe oligonucleotides listed in Table 1. Solutions were prepared as 1.0 and 0.06 μM in green and red QD-conjugates, respectively, in TB buffer with the desired equivalents of labeled target. Solutions were allowed to stand at room temperature for 7–8 h prior to measurement. Measurements on the red system were obtained with a 615 nm long-pass coloured glass filter (Melles-Griot). The green system required no optical filtering.

For multi-colour experiments, green QD–1 × DNA and red QD–2 × DNA conjugates were prepared as a mixture in TB buffer with 1.0 and 0.06 μM concentrations, respectively. Targets were introduced at the desired concentrations and the solutions were allowed to stand for 7–8 h prior to measurement.

Both single-colour and two-colour luminescence spectra were acquired using 396 nm excitation and TB buffer served as the blank. Direct excitation of Cy3 is minimized at 385 nm and direct excitation of Alexa647 is minimized at 425 nm. The minimum additive emission from direct excitation with a mixture of the two dyes was found at 396 nm. In these experiments, direct excitation of either dye at 396 nm at any of the concentrations used was not distinguishable from the background within the experimental precision.

Single-colour experiments with ethidium bromide were conducted similarly to those described above, except that the target oligonucleotides were unlabeled and 6 equiv. of ethidium bromide were added after the hybridization period. The ethidium bromide was allowed to equilibrate 3–4 h prior to measurement. Experiments involving mixtures of target and dA_{20} oligonucleotides or salmon sperm DNA were conducted similarly, except for the additional nucleic acid material. In contrast to Cy3 and Alexa647, the direct excitation of ethidium bromide was detectable. The excitation wavelength was selected to be 400 nm were the lowest direct excitation of ethidium bromide was observed compared to other excitation wavelengths.

3. Results and discussion

3.1. Characterization of quantum dots and QD–DNA conjugates

Changes in QD quantum yield associated with ligand exchange and DNA conjugation are given in Table 2. The quantum yield of the QDs decreased by roughly an order of magnitude between the organic and aqueous systems, and further changed upon DNA conjugation. A 2 nm shift to longer wavelengths was observed in the emission of the green QDs between organic and aqueous phases. While not listed in Table 2, it was also found that increasing the number of probes per green QD from one to two approximately doubled the quantum yield. Similarly, an approximate two-fold increase in quantum yield was also observed when there were six probes per red QD rather than two. These results suggest that the conjugation of DNA helps passivate the QD surface and improve quantum yield, but that the effect may be partially counteracted by the additional purification process associated with removal of excess EDC. The quantum yield of the water soluble QDs and QD–DNA conjugates appeared to vary significantly between preparations. The uncertainties listed in Table 2 represent the variability between different batch preparations. Replicate measurements of samples from a single batch show variation in the range of 0.1–4%. Given the well-known instability of thiol capped QDs in aqueous solution, it is not surprising that the quantum yield was sensitive to the nature of the preparation. It is suspected that the purification steps are the main source of the variability since the equilibrium between bound and unbound thiol is disrupted and not re-established until the final dispersion in Tris–borate (TB) buffer.

Table 2
Quantum yields and Förster distances of QDs

QD colour	Quantum yield ($\times 10^{-2}$)			Förster distance (nm)	
	QDs (toluene)	MAA–QDs (aq.)[b]	QD–DNA conjugate (aq.)[c]	Cy3	Alexa647
Green[a]	28.6 ± 0.8 (524 nm)	1.8 ± 0.6 (526 nm)	0.4 ± 0.2 (526 nm)	2.7 ± 0.2	–
Red[a]	9.2 ± 0.4 (606 nm)	0.4 ± 0.1 (606 nm)	0.9 ± 0.6 (606 nm)	–	3.52 ± 0.2

[a] The position of the emission maximum, λ_{max}, is given in parentheses.
[b] Water soluble QDs with mercaptoacetic acid ligands.
[c] The green QD have a single conjugated oligonucleotide; the red QDs have two conjugated oligonucleotides.

3.2. Single-colour hybridization assays with Cy3 and Alexa647

A hybridization event between a QD–DNA conjugate and a dye-labeled complementary sequence of DNA brought the dye label within a distance on the order of the Förster radius of the QD–dye FRET pair. As a consequence, FRET-sensitized dye fluorescence was observed. In these experiments, green and red emitting CdSe/ZnS core-shell QDs were used as energy donors with Cy3 and Alexa647 labeled oligonucleotides as energy acceptors. The absorption and emission spectra for these QDs and dyes are shown in Fig. 2.

Hybridization between probe and target has been confirmed experimentally in a number of ways. Significant differences in the kinetic rates of hybridization and non-specific adsorption using a non-complementary sequence were observed, and fluorescence spectra obtained using PicoGreen to stain double stranded DNA indicated the formation of hybrids (see Supplementary Information). Similarly, ethidium bromide demonstrated the expected fluorescence lifetime of *ca.* 20 ns (characteristic of the presence of dsDNA) when QD–DNA conjugates were mixed with complementary material. Melt curves were also obtained with QD–DNA conjugates demonstrating dehybridization as a function of temperature.

The hybridization-FRET-sensitized fluorescence of both Cy3 and Alexa647 labeled targets is shown in Fig. 3 as a function target concentration. In Fig. 3a, solutions containing green QD with one conjugated SMN1 probe oligonucleotide (green QD–1 × DNA) were exposed to different amounts of SMN1 target. In Fig. 3b, solutions containing red QD with two conjugated LacZ oligonucleotide probes (red QD–2 × DNA) were exposed to different amounts of LacZ target. In both cases, the acceptor fluorescence was observed to increase with increasing target hybridization. The fluorescence intensity in the Cy3 spectral region was linear at target concentrations ≥400 nM and varied predictably at lower concentrations. For a 1.0 μM concentration of QD–DNA conjugate, the limit-of-detection (LOD) is estimated to be 40 nM using the definition of three standard deviations above the baseline in the absence of target. The fluorescence intensity in the Alexa647 spectral region was found to change linearly at all target concentrations, with an estimated LOD of 12 nM for a QD–DNA conjugate concentration of 0.06 μM. For both colours, the upper limit of the dynamic range was defined by the concentration of the QD–DNA conjugate. The different LODs between the green and red systems demon-

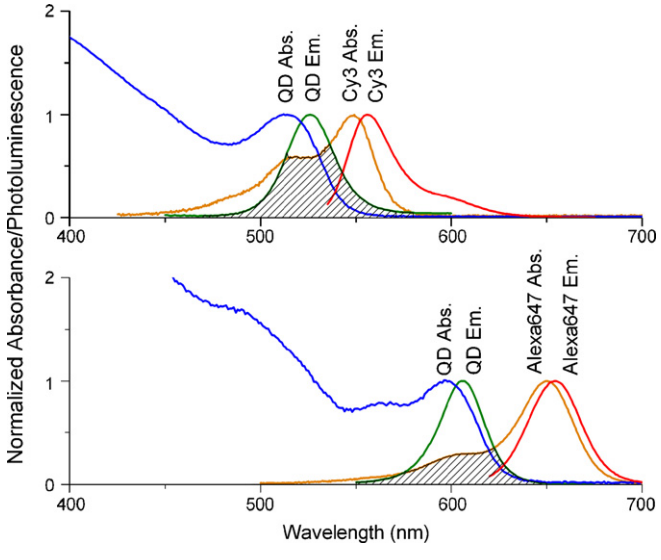

Fig. 2. Spectral overlap (shaded) for the two FRET systems of interest: (a) a green QD donor with a Cy3 labeled acceptor and (b) a red QD with an Alexa647 labeled acceptor. Both the normalized absorption (abs.) and emission (em.) spectra are shown. Note that the absorption coefficient for the red QD is approximately an order of magnitude larger than for the green QD. (For interpretation of the references to colour in this figure legend, the reader is referred to the web version of the article.)

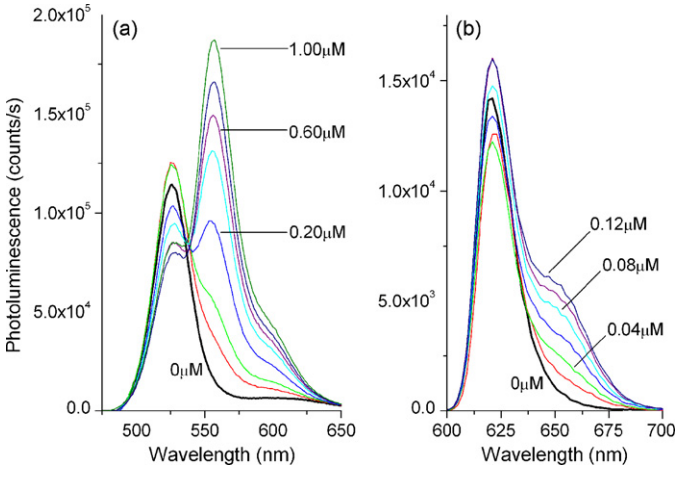

Fig. 3. Single-colour experiments demonstrating the ability to quantitatively detect labeled target oligonucleotide sequences via FRET-sensitized emission: (a) a 1.0 μM solution of green QD–1 × DNA conjugate with 80, 100, 200, 400, 600, 800, and 1000 nM of Cy3-labeled target; (b) a 0.06 μM solution of red QD–2 × DNA conjugate with 20, 40, 60, 80, 100, and 120 nM of Alexa647-labeled target.

strate that the lower limit of the dynamic range, and thus LOD, is a function of the amount of QD–DNA conjugate. Although the dynamic range is small at one particular concentration of conjugate, it is effectively tunable over a range of QD–DNA conjugate concentrations. For example, a reduction in green QD concentration of two orders of magnitude is still detectable in a simple spectrofluorimeter and provides picomolar LODs. In addition, FRET between quantum dots and organic dyes has been shown to be detectable at the single molecule level [36], suggesting that this diagnostic methodology could be extended to such a platform. In terms of ensemble measurements, any lack of sensitivity compared to other techniques may be offset by this resistance of this scheme to photobleaching, making it ideal for a continuous monitoring biosensor application.

It should be noted that the difference in concentration between the green and red systems is required to give similar QD luminescence intensities. In addition, the quantum yield of the Alexa647 dye was less than that of Cy3 in this experiment. As a consequence of these two factors, the large photoluminescence from the red QD largely obscured the FRET-sensitized shoulder from Alexa647 emission. However, it was possible to reduce the emission contribution of the red QD with the addition of a 615 nm long-pass glass filter. This had the effect of shifting the apparent emission maximum from 606 to 620 nm (see Supplementary Material for spectra). All FRET-related steady state data were obtained in this manner and the red shift of the QD emission maximum in Fig. 3 relative the unfiltered emission in Fig. 2 is a consequence of this effect.

Photoluminescence lifetimes measured for the QD–DNA conjugates are listed in Table 3 and may be compared to the lifetimes measured for green (7.0 ± 0.2 ns) and red (8.4 ± 0.2 ns) MAA–QDs. Changes in lifetime and relative quantum yield associated with the hybridization of an unlabeled complementary target oligonucleotide (QD–$n \times$ dsDNA) were observed. The increase in quantum yield upon hybridization is consistent with the aforementioned increase in quantum yield with a greater number of conjugated probe oligonucleotides. The standard deviations reported in Table 3 are associated with measurements using a single batch preparation of QD–DNA conjugates. Since the quantum yield and lifetime may change with the nuances of each conjugate preparation, it is not the absolute values which are of interest, but rather the relative change in those values. It is important to note that the changes in quantum yield and lifetime observed in Table 3 are associated entirely with the hybridization process since there is no clean-up step (as done with probe conjugation with EDC).

The FRET efficiencies observed for the green and red systems are 52 and 6.7%. These values were calculated from the data in Table 3 by comparing the lifetimes (and relative quantum yields) for QD–$n \times$ dsDNA and QD–$n \times$ dsDNA–acceptor dye. The relationships between FRET efficiency, E, and lifetime, τ, or quantum yield, Φ, are given by Eq. (4), where DA indicates a donor quantity (D) in the presence of n acceptors (A). The efficiencies calculated from the lifetime/quantum yield data are listed in Table 3, and allow the donor–acceptor separation, r, to be determined from Eq. (5). The Förster distances, R_o, are listed in Table 2. The R_o values are calculated from spectra and the quantum yields for QD–DNA conjugate, based on a buffer refractive index of 1.34 and an assumed orientation factor of $\kappa^2 = 2/3$. This last approximation has been shown to be valid when the orientation of both the quantum dot exciton and the acceptor transition dipole are expected to be at least partially randomized [37]. The spectral overlaps determined for the green QD–Cy3 and red QD–Alexa647 pairs are $(5.0 \pm 0.4) \times 10^{-10}$ cm^6 and $(1.14 \pm 0.07) \times 10^{-9}$ cm^6, respectively. The donor–acceptor distances calculated from Eqs. (4) and (5), and the lifetime (or quantum yield) data are 2.7 nm (or 2.5 nm) and 6.1 nm (or 5.6 nm), respectively. These values are quite reasonable considering the hydrodynamic radius of DNA, the QD dimensions (green QD: 2.1 nm core diameter; red QD: 5.2 nm core diameter [38]), and assuming the DNA adopts some conformation along the surface of the QD. Given the large size of the red QD, it is not surprising that the FRET efficiency is much higher in the green system.

$$E = 1 - \frac{\tau_{DA}}{\tau_D} = 1 - \frac{\Phi_{DA}}{\Phi_D} \tag{4}$$

$$E = \frac{n R_o^6}{n R_o^6 + r^6} \tag{5}$$

3.3. Simultaneous two-colour hybridization assay with Cy3 and Alexa647

The single-colour green and red QD systems were successfully integrated into a two-colour detection scheme as shown in Fig. 4. The FRET-sensitized signals in the Cy3 and Alexa647 emission windows were observed to change as a function of the quantity of target material. Fig. 4(a) shows the change in FRET

Table 3
FRET efficiency derived from changes in quantum yield and photoluminescence lifetime

Green system[a]	Lifetime (ns)	Relative QY[b]	Red system[a]	Lifetime (ns)	Relative QY[b]
QD–1 × DNA	8.5 ± 0.3	1.00 ± 0.05	QD–2 × DNA	6.2 ± 0.2	1.00 ± 0.03
QD–1 × dsDNA	8.7 ± 0.3	1.31 ± 0.01	QD–2 × dsDNA	5.9 ± 0.1	1.34 ± 0.03
QD–1 × dsDNA–Cy3	4.4 ± 0.1	0.48 ± 0.03	QD–2 × dsDNA–Alexa647	5.5 ± 0.1	1.18 ± 0.18
FRET efficiency (%)[c]	52 ± 3	63 ± 3	FRET efficiency (%)[c]	6.7 ± 0.2	11 ± 2

[a] QD–$n \times$ DNA represents QDs with n conjugated oligonucleotide probes, which may by hybridized with target as indicated by "dsDNA". The target may also be fluorophore labeled, as indicated.
[b] Relative quantum yield.
[c] FRET efficiency as a percentage.

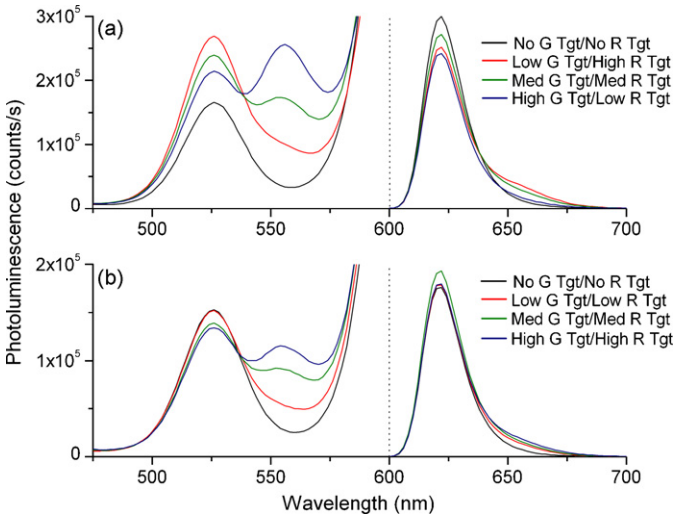

Fig. 4. Two-colour experiments demonstrating the ability to quantitatively detect two different labeled oligonucleotide sequences simultaneously via FRET-sensitized emission: (a) 1.0 and 0.06 μM solution of gQD–1 × DNA and rQD–2 × DNA, respectively, with: no targets, 330 nM Cy3-target + 120 nM Alexa647-target, 660 nM Cy3-target + 80 nM Alexa647 target, and 1000 nM Cy3-target + 40 nM Alexa647-target; (b) 1.0 and 0.06 μM solution of gQD–1 × DNA and rQD–2 × DNA, respectively, with: no targets, 330 nM Cy3-target + 40 nM Alexa647-target, 660 nM Cy3-target + 80 nM Alexa647 target, and 1000 nM Cy3-target + 120 nM Alexa647-target. The green and red systems appeared to change independently. Channels are delineated by the dashed line at 600 nm.

signals when the green target concentration is increased and red target concentration is simultaneously decreased. Fig. 4(b) shows the change in FRET signals when both the green and red target concentrations are simultaneously increased. Comparing Fig. 4(a) and (b), it is observed that the FRET-sensitized signals changed independently of one another. The data clearly demonstrates the capacity for a two-colour detection scheme. The data in Fig. 4 also shows that 1.0 and 0.06 μM concentrations of green and red QD–DNA conjugate were able to detect target concentrations in the range of 10^{-1} to 10^{0} μM and 10^{1} to 10^{2} nM, respectively. However, it should again be noted that the dynamic range of either single-colour system can be tuned by changing the quantity of QD-conjugate and is limited only by the ability to resolve the four emission components and the effects of non-specific adsorption (discussed in Section 3.4).

3.4. Non-specific adsorption

Non-specific adsorption of oligonucleotides has been found to be very strong on MAA–QDs and only slightly reduced with QD–DNA conjugates. The FRET signal may be semi-quantitatively treated as the ratio of the emission intensity at the Cy3 emission maximum to the intensity at the green QD maximum. Ratios of roughly 0.1, 1.8, and 1.0 were obtained for green QD–1 × DNA, green QD–1 × DNA hybridized with fully complementary target, and green QD–1 × DNA with adsorbed non-complementary target, respectively, indicating a signal-to-noise ratio less than two (S/N < 2). The red QD–2 × DNA system showed slightly stronger non-specific adsorption, likely due to the larger surface area available. In an effort to prevent non-specific adsorption of oligonucelotides, maintain quantum yield, and allow facile hybridization, the use of bovine serum albumin (BSA), polyvinyl pyrrolidone (PVP), poly-L-lysine as blocking agents, or additions of Tween 20 or a small percentage of formamide were explored. Only BSA was successful in preventing non-specific adsorption, but the hybridization signal from complementary target was found be greatly reduced.

An interesting aspect seen in Fig. 4 is that the Cy3 and Alexa647 FRET signals in the two-colour experiments were less than those observed in the single-colour experiments. Although the hybridization signals changed independently with target concentration, this result may indicate that there was interaction between the two systems. Non-specific adsorption in the two-colour system was observed to be less that that seen in the single-colour experiments. Although the green QDs were approximately ≥17-fold more concentrated than the red quantum dots, the ratio of red-to-green QD surface area is >6 (based on core diameter) and could have helped offset the concentration difference. Adsorption of red target on green quantum dots and vice versa could not be directly detected due to the absence of significant spectral overlap, however, the effect may be observable as the reduction of the red signal associated with hybridization. As can be seen by comparing Fig. 4 with Fig. 3, adsorption of green target onto red QDs appears to have less effect on the spectra. The different extents of the cross-adsorption effects on the green (smaller effect) and red (larger effect) channels were likely due, in part, to the concentration difference in target oligonucleotides. As shown in Fig. 5, preliminary experiments also demonstrate that the hybridization kinetics of the red QD–probe conjugates were substantially faster than the green QD–probe conjugates, allowing red probe–target hybridization on the red QDs to partially offset the adsorption of red target on the green QDs. As

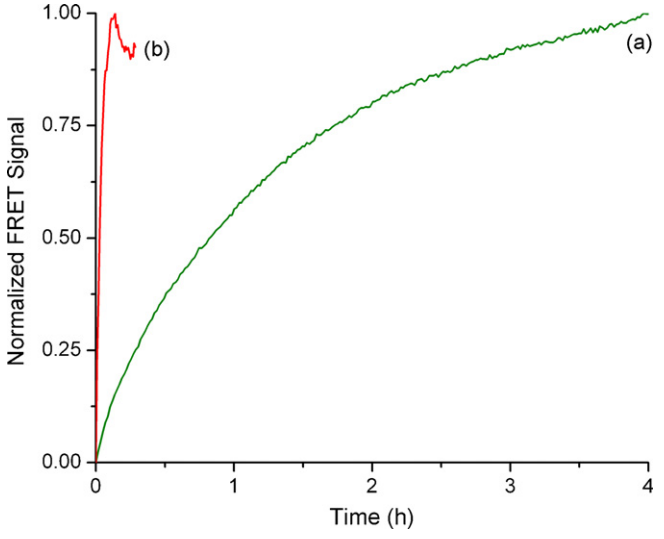

Fig. 5. Normalized kinetic traces for the evolution of FRET-sensitized Cy3 fluorescence (at 560 nm) from (a) 1.0 μM complementary target with 1.0 μM of green QD–1 × DNA conjugate and (b) 0.12 μM complementary target with 0.06 μM of red QD–2 × DNA conjugate. Note the much faster kinetics of (b) relative (a). (For interpretation of the references to colour in this figure legend, the reader is referred to the web version of the article.).

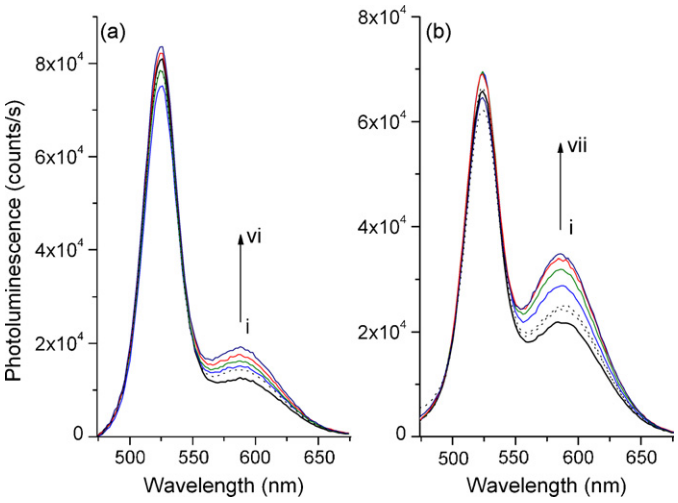

Fig. 6. Experiments demonstrating the ability to detect labeled target oligonucleotide sequences via FRET-sensitized ethidium bromide emission: (a) a 1.0 μM solution of green QD–1 × DNA conjugate with 6.0 μM ethidium bromide and (i) 0.0 μM target, (ii) 1.0 μM non-complementary sequence, (iii) 0.2 μM target, (iv) 0.4 μM target, (v) 0.6 μM target, (vi) 1.0 μM target; (b) a 1.0 μM solution of green QD–2 × DNA conjugate with 12.0 μM ethidium bromide and (i) 0.0 μM target, (ii) 2.0 μM non-complementary sequence, (iii) 4.0 μM non-complementary, (iv) 0.8 μM target, (v) 1.2 μM target, (vi) 1.6 μM target, (vii) 2.0 μM target. In (a), the curve for 2.0 μM of non-complementary target has been omitted for clarity, but is only 3% greater than that for 0.2 μM target. The curve for 0.4 μM target in (b) has also been omitted for clarity. Curves for non-complementary material are shown as dashed lines. The data suggests the signal associated with hybridization is 9–10-fold larger than that of an equal amount of non-complementary material. (For interpretation of the references to colour in this figure legend, the reader is referred to the web version of the article.)

a consequence, the red FRET signals in the two-colour system are not completely diminished.

3.5. Hybridization assay with ethidium bromide

Ethidium bromide is an intercalating dye which shows a strong enhancement of quantum yield upon incorporation into double-stranded DNA, but shows much weaker fluorescence in the presence of single-stranded DNA. Fig. 6 shows hybridization assays with green QD systems: (a) 1.0 μM of green QD–1 × DNA with the addition of variable amounts of non-labeled target or non-complementary sequence and 6 equiv. of ethidium bromide; (b) 1.0 μM of green QD–2 × DNA with variable amounts of target or non-complementary sequence and 12 equiv. of ethidium bromide (i.e. 6 equiv. per probe). The figures also show the direct excitation of ethidium bromide associated with the system in the absence of target. Six equivalents of ethidium bromide allows the maximum acceptor absorption cross-section for FRET (as per Eq. (5)) while ensuring that the intercalative capacity of the 19-base SMN1 sequence is not exceeded. The use of multiple equivalents also helps offset the lower quantum yield and molar absorption coefficient of ethidium bromide as compared to Cy3. As observed in Fig. 6, increasing FRET-sensitized ethidium bromide emission with increasing target is observed and signal-to-noise is greatly increased with respect to non-specific adsorption, reaching a value of S/N = 9–10. This is seen in Fig. 6a, where the signal from 1.0 equiv. of non-complementary material is less than that observed with 0.2 equiv. of target. In addition, the signal associated with 2.0 equiv. of non-complementary material is equal (within experimental precision) to that observed with 0.2 equiv. of target, suggesting the upper limit of S/N. Similar S/N is observed with the green QD–2 × DNA system shown in Fig. 6b. In this case, the signal from 4.0 equiv. of non-complementary material equal to the signal expected for 0.4 equiv. of target. The estimated LOD for the green QD–1 × DNA–ethidium bromide system is 80 nM at a QD-conjugate concentration of 1.0 μM. The estimated LOD for the green QD–2 × DNA–ethidium bromide system is 165 nM. The upper limits of the dynamic ranges are 1.0 and 2.0 μM, respectively. Due to the lower quantum yield of ethidium bromide relative Cy3, the tunability of the dynamic range is roughly an order of magnitude less than that associated with Cy3. The system has been tested against matrices containing a six-fold excess of non-complementary dA_{20} oligonucleotide and 10-fold excess of salmon sperm DNA. The hybridization signals were approximately 80 and 100% of that associated with clean matrices, respectively.

Lifetime measurements suggest that the FRET efficiencies for the QD–ethidium bromide systems are approximately 5%. The lower efficiency compared with Cy3 is due to the much lower molar absorption coefficient of ethidium bromide. The calculated Förster distance for the green QD–ethidium bromide pair is 1.82 ± 0.08 nm. With judicious choice of a second intercalating dye, it should be possible to construct a two-colour intercalating dye system similar to that demonstrated with Cy3 and Alexa647, but less sensitive to non-specific adsorption. Dyes potentially suitable for use with the red QD include TO-PRO-3 and YO-PRO-3, which both have spectrally resolved emission from the red QD and absorption shoulders in overlap with the red QD emission. However, since these dyes have no sequence selectivity, each probe/target hybrid would have mixture of acceptors. This would not result in spurious FRET signals since only one dye will have significant spectral overlap with the donor, but a reduction in overall signal intensity would occur. The use of probe-tethered intercalating dyes [39–41] would address this issue. As discussed previously with respect to the Cy3 and Alexa647 labeled targets, moving the scheme to a single-molecule platform to improve sensitivity should be feasible. Similarly, in a continuous monitoring biosensor scheme, the QD–ethidium bromide FRET system should remain substantially more resistant to photobleaching than in a direct excitation scheme.

4. Conclusions

The potential for both single- and two-colour diagnostic schemes for nucleic acid hybridization based on FRET between quantum dot donors and acceptor fluorophore labeled oligonucleotides has been demonstrated. The single-colour schemes were quantitative, where FRET-sensitized acceptor fluorescence was observed to change systematically as a function of target concentration. The dynamic range is tunable with the concentration of QD–DNA conjugate (within the limits of available

instrument). Results show that the green QD–Cy3 pair can detect target as low as 4% as the QD concentration. The red QD–Alexa647 pair can detect target as low as 10% of the QD concentration. The green QD–ethidium bromide pair can detect target as low as 8% of the QD concentration. In all cases, the upper limit of the dynamic range is defined by the QD concentration. In the two-colour scheme, the colours responded proportionately to target concentration and relatively independently of one another, although with reduced signals relative the single-colour system. This was a consequence of non-specific adsorption, which was not preventable with standard blocking agents. To alleviate the effects of non-specific adsorption, the use of an intercalating dye (ethidium bromide) as an acceptor was demonstrated. Signal-to-noise with respect to hybridization and non-specific adsorption increased from S/N < 2 with the Cy3 or Alexa647 systems to S/N = 9–10 with ethidium bromide. The ethidium bromide system was also found to effectively detect target in a matrix containing an excess of non-complementary oligonucleotide or salmon sperm DNA.

Acknowledgements

The authors acknowledge the Natural Sciences and Engineering Research Council of Canada (NSERC) for financial support of this work and provision of a fellowship to WRA. The authors also thank Prof. Virginijus Barzda, Dr. Arkady Major, and Dr. Paul Piunno for the use of their instrumentation and assistance in acquiring the lifetime data.

Appendix A. Supplementary data

Supplementary data associated with this article can be found, in the online version, at doi:10.1016/j.aca.2006.08.026.

References

[1] M. Han, X. Gao, J.Z. Su, S. Nie, Nat. Biotechnol. 19 (2001) 631.
[2] J.K. Jaiswal, H. Mattoussi, J.M. Mauro, S.M. Simon, Nat. Biotechnol. 21 (2003) 47.
[3] M. Stroh, J.P. Zimmer, D.G. Duda, T.S. Levchenko, K.S. Cohen, E.B. Brown, D.T. Scadden, V.P. Torchilin, M.G. Bawendi, D. Fukumura, R.K. Jain, Nat. Med. 11 (2005) 678.
[4] A.M. Smith, X. Gao, S. Nie, Photochem. Photobiol. 80 (2004) 377.
[5] I.L. Medintz, H.T. Uyeda, E.R. Goldman, H. Mattoussi, Nat. Mater. 4 (2005) 435.
[6] F. Pinaud, X. Michalet, L.A. Bentolila, J.M. Tsay, S. Doose, J.J. Li, G. Iyer, S. Weiss, Biomaterials 27 (2006) 1679.
[7] E.R. Goldman, A.R. Clapp, G.P. Anderson, H.T. Uyeda, J.M. Mauro, I.L. Medintz, H. Mattoussi, Anal. Chem. 76 (2004) 684.
[8] E.R. Goldman, I.L. Medintz, J.L. Whitley, A. Hayhurst, A.R. Clapp, H.T. Uyeda, J.R. Deschamps, M.E. Lassman, H. Mattoussi, J. Am. Chem. Soc. 127 (2005) 6744.
[9] J.H. Kim, D. Morikis, M. Ozkan, Sens. Actuators B 102 (2004) 314.
[10] C.Y. Zhang, H.C. Yeh, M.T. Kuroki, T.H. Wang, Nat. Mater. 4 (2005) 826.
[11] R. Gill, I. Willner, I. Shweky, U. Banin, J. Phys. Chem. B 109 (2005) 23715.
[12] D. Zhou, J.D. Piper, C. Abell, D. Klenerman, D.J. Kang, L. Ying, Chem. Comm. (2005) 4807.
[13] E. Chang, J.S. Miller, J. Sun, W.W. Yu, V.L. Colvin, R. Drezek, J.L. West, Biochem. Biophys. Res. Commun. 334 (2005) 1317.
[14] I.L. Medintz, A.R. Clapp, H. Mattoussi, E.R. Goldman, G. Fisher, J.M. Mauro, Nat. Mater. 2 (2003) 630.
[15] A. Almadidy, J. Watterson, P.A.E. Piunno, S. Raha, I.V. Foulds, P.A. Horgen, A. Castle, U. Krull, Anal. Chim. Acta 461 (2002) 37.
[16] S. Ahn, D.R. Walt, Anal. Chem. 77 (2005) 5041.
[17] J.H. Watterson, S. Raha, C.C. Kotoris, C.C. Wust, F. Gharabaghi, S.C. Jantzi, N.K. Haynes, N.H. Gendron, U.J. Krull, A.E. Mackenzie, P.A.E. Piunno, Nucl. Acids Res. 32 (2004) e18.
[18] I. Biran, D.R. Walt, Anal. Chem. 74 (2002) 3046.
[19] M. Schena, D. Shalon, R.W. Davis, P.O. Brown, Science 270 (1995) 467.
[20] A.E. Warsen, M.J. Krug, S. LaFrentz, D.R. Stanek, F.J. Loge, D.R. Call, Appl. Environ. Microbiol. 70 (2004) 4216.
[21] M.J. Hessner, X. Wang, K. Hulse, L. Meyer, Y. Wu, S. Nye, S.W. Guo, S. Ghosh, Nucl. Acids Res. 31 (2003) e14.
[22] X. Zhou, J. Zhou, Anal. Chem. 76 (2004) 5302.
[23] R.Q. Liang, W. Li, Y. Li, C. Tan, J.X. Li, Y.X. Jin, K.C. Ruan, Nucl. Acids Res. 33 (2005) e17.
[24] J.S. Shumaker-Parry, M.H. Zareie, R. Aebersold, C.T. Campbell, Anal. Chem. 76 (2004) 918.
[25] S.J. Chen, Y.D. Su, F.M. Hsiu, C.Y. Tsou, Y.K. Chen, J. Biomed. Opt. 10 (2005) 034005.
[26] E. Rockenbauer, K. Petersen, U. Vogel, L. Bolund, S. Kølvraa, K.V. Nielsen, B.A. Nexø, Cytometry 64A (2005) 80.
[27] R.J. Fulton, R.L. McDade, P.L. Smith, L.J. Kienker, J.R. Kettman, Clin. Chem. 43 (1997) 1749.
[28] H. Xu, M.Y. Sha, E.Y. Wong, J. Uphoff, Y. Xu, J.A. Treadway, A. Truong, E. O'Brien, S. Asquith, M. Stubbins, N.K. Spurr, E.H. Lai, W. Mahoney, Nucl. Acids Res. 31 (2003) e43.
[29] X. Gao, S. Nie, Anal. Chem. 76 (2004) 2406.
[30] L. Wang, W. Tan, Nano Lett. 6 (2006) 84.
[31] A.R. Clapp, I.L. Medintz, H.T. Uyeda, B.R. Fisher, E.R. Goldman, M.G. Bawendi, H. Mattoussi, J. Am. Chem. Soc. 127 (2005) 18212.
[32] J. Aldana, Y.A. Wang, X. Peng, J. Am. Chem. Soc. 123 (2001) 8844.
[33] H. Matoussi, J.M. Mauro, E.R. Goldman, G.P. Anderson, V.C. Sundar, F.V. Mikulec, M.G. Bawendi, J. Am. Chem. Soc. 122 (2000) 12142.
[34] H.C. Cheung, Topics in Fluorescence Spectroscopy. Vol. 2: Principles, Plenum Press, New York, 1991.
[35] R. Sjöback, J. Nygren, M. Kubista, Spectrochim. Acta A 51 (1995) L7.
[36] S. Hohng, T. Ha, ChemPhysChem 6 (2005) 956.
[37] A.R. Clapp, I.L. Medintz, J.M. Mauro, B.R. Fisher, M.G. Bawendi, H. Mattoussi, J. Am. Chem. Soc. 126 (2004) 301.
[38] Evident Technolgies, 2006. http://www.evidenttech.com/nanomaterials/evidots/quantum-dot-specifications.php.
[39] X.F. Wang, U.J. Krull, Anal. Chim. Acta 470 (2002) 57.
[40] X.F. Wang, U.J. Krull, Bioorg. Med. Chem. Lett. 15 (2005) 1725.
[41] X.F. Wang, U.J. Krull, J. Mater. Chem. 15 (2005) 2801.